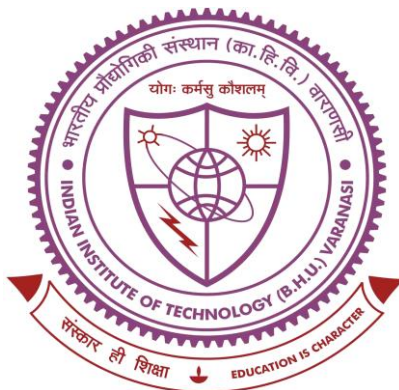


SYNTHESIS OF CARBON BASED FLUORESCENT NANOMATERIALS AND THEIR APPLICATIONS



THESIS SUBMITTED IN PARTIAL FULFILLMENT
FOR THE AWARD OF DEGREE

DOCTOR OF PHILOSOPHY

By

Subhash Chandra

Department of Chemistry
Indian Institute of Technology
(Banaras Hindu University)
Varanasi- 221005

Roll No. 17051012

2022

CERTIFICATE

It is certified that the work contained in the thesis titled "*Synthesis of carbon based fluorescent nanomaterials and their applications*" by "*Subhash Chandra*" has been carried out under my supervision and this work has not been submitted elsewhere for a degree.

It is further certified that the student has fulfilled all the requirements of Comprehensive, Candidacy and SOTA.

hadi

Prof. Syed Hadi Hasan
(Supervisor)
Department of Chemistry,
Indian Institute of Technology
(Banaras Hindu University),
Varanasi-221005

Dr. S. H. Hasan
Professor
Department of Chemistry
Indian Institute of Technology (B.H.U.)
Varanasi-221005

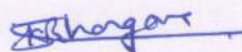
Am
Convener, DPGC of the
Department/School
DPGC
Indian Institute of Technology (B.H.U.)
Varanasi-221005

DECLARATION BY THE CANDIDATE

I, "Subhash Chandra", certify that the work embodied in this thesis is my own bonafide work and carried out by me under the supervision of "Prof. Syed Hadi Hasan" from "July 2017" to "August 2022", at the "Department of Chemistry", Indian Institute of Technology (BHU), Varanasi. The matter embodied in this thesis has not been submitted for the award of any other degree/diploma. I declare that I have faithfully acknowledged and given credits to the research workers wherever their works have been cited in my work in this thesis. I further declare that I have not wilfully copied any other's work, paragraphs, text, data, results, etc., reported in journals, books, magazines, reports dissertations, theses, etc., or available at websites and have not included them in this thesis and have not cited as my own work.

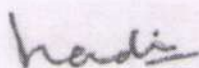
Date: 08/08/2022

Place: Varanasi


Subhash Chandra

CERTIFICATE BY THE SUPERVISOR

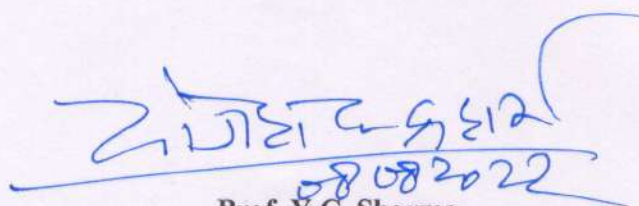
It is certified that the above statement made by the student is correct to the best of my knowledge.



Prof. Syed Hadi Hasan
(Supervisor)

Department of Chemistry
Indian Institute of Technology
(Banaras Hindu University)
Varanasi- 221005

Dr. S. H. Hasan
Professor
Department of Chemistry
Indian Institute of Technology (B.H.U.)
Varanasi-221005


08/08/2022

Prof. Y.C. Sharma

Head of Department

Department of Chemistry,
Indian Institute of Technology
(Banaras Hindu University),
Varanasi- 221005

विभागाध्यक्ष / HEAD

रसायन विज्ञान विभाग

Department of Chemistry
भारतीय प्रौद्योगिकी संस्थान (का.हि.वि.दि.)
Indian Institute of Technology (B.H.U.)
वाराणसी-221005/Varanasi

COPYRIGHT TRANSFER CERTIFICATE

Title of the Thesis: *Synthesis of carbon based fluorescent nanomaterials and their applications*

Name of the Student: *Subhash Chandra*

Copyright Transfer

The undersigned hereby assigns to the Indian Institute of Technology (Banaras Hindu University), Varanasi, all rights under copyright that may exist in and for the above thesis submitted for the award of the "*Doctor of Philosophy.*"

Date: *08/08/2022*

Place: Varanasi



Subhash Chandra

Note: However, the author may reproduce or authorize others to reproduce material extracted verbatim from the thesis or derivative of the thesis for author's personal use provided that the source and the Institute's copyright notice are indicated.

Dedicated to My Beloved
PARENTS

Acknowledgement

It is indeed my proud privilege to express my deep sense of gratitude and indebtedness to my supervisor, Dr. S. H. Hasan, HAG Professor, Department of Chemistry, Indian Institute of Technology (BHU), Varanasi for his enormous help, co-operation and valuable supervision that he has extended to me for the successful completion of this investigation. I am indebted to him for his consistent encouragement, sustained interest and parental care throughout the research period.

I am obliged very much to express my sincere thanks to HOD, Prof. Y.C. Sharma and Ex HOD, Prof. D. Tiwary and Prof. R. B. Rastogi, Department of Chemistry, Indian Institute of Technology (BHU) for providing necessary facilities and constant motivation throughout my research work.

It is my pleasure to express my cheers to all RPEC members Prof. S.K. Shrivastava, Department of Pharmaceutical Engineering and Technology, IIT (BHU), Dr. Asha Gupta, Department of Chemistry, IIT (BHU). Their numerous insight and generous assistance helped me significantly in improving my research work. They always came forward to assist me whenever I needed.

My passionate thanks go to all the faculty members, Department of Chemistry IIT (BHU) for their support and encouragement.

I constraint special thanks for all the non-teaching staff of the Department of Chemistry, IIT (BHU) as this work would have never been completed without their technical support.

I also gratefully acknowledge to the Ministry of Human Resource and Development (MHRD), Govt. of India, New Delhi, and Director, IIT (BHU) for the financial support in the form of teaching assistantship.

I am blessed to have very supportive and caring labmates Mr. Pradeep Kumar Yadav, Mr. Vivek Kumar, and Mr. Deepak Kumar for their valuable support and encouragement towards the successful completion of my research work.

I am gratified to express my sincere thanks to my lab seniors Dr. Vijay Kumar, Dr. Sweta Mohan, and Dr. Devendra Kumar Singh, Dr. Vikas Kumar Singh, Dr. Vinay Kumar pandey

Acknowledgement

and Dr. Daraksha Bano Department of Chemistry, IIT (BHU) for their encouragement and valuable suggestions during my research period.

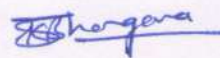
I would like to thank my friends and senior Dr. Bharat kumar, Dr. Gitanjali Pradhan, Dr. Kedar Sahoo, Dr. Ravi Kumar Sonwani, Mr, Murli Dhar Mitra, Mr. Ved Vyas, Mr. Abhimanyu Yadav, Dr. Ravindra Kumar Gautam, Dr. Atendra Kumar, and Dr. Shiva Sundar Yadava for making my PhD journey happy.

I am also grateful to my friends Dr. Saroj Kumar BBAU Lucknow, Mr. Vishnu Kumar Modanwal, University of Allahabad, and Dr. Arvind Kumar Pandey, University of Allahabad for their valuable support throughout my PhD work.

I wish to express my vivid thanks to Ms, Simpal Gond for always encouraging and motivating me during my research work.

I wish to acknowledge all those, who helped me in any form during the entire period of my research work.

Last but not least I am grateful to my family members for their blessings, cooperation, sacrifices, encouragement and patience. It's been possible with the blessings of my father, Late. Mr. Deen Dayal and untiring efforts and prayers of my mother, Mrs. Santa Devi that provided me all the wisdom, strength and guidance to carry on this journey which at times became very harsh and monotonous.



Subhash Chandra

Contents

Title	Page No.
TITLE OF THESIS	i
CERTIFICATE	ii
DECLARATION BY THE CANDIDATE & CERTIFICATE BY THE SUPERVISOR	iii
COPYRIGHT TRANSFER CERTIFICATE	iv
Dedication	v
Acknowledgement	vi-vii
Contents	viii-xiv
List of Figures	xv-xix
List of Schemes	xx
List of Tables	xxi
List of Symbols/Abbreviations	xxii-xxiv
Preface	xxv-xxviii
Chapter 1: Introduction and literature review	1-36
1.1 Introduction	1
1.2 Carbon quantum dots (CQDs)	5
1.2.1 Synthesis of CQDs	6
1.2.1.1 Top-down approach	7
A. Laser Ablation	8
B. Arc-discharge method	8
C. Electrochemical method	9
1.2.1.2 Bottom-up Approach	9
A. Thermal oxidation/Combustion method	10
B. Microwave Irradiation method	10

C.	Ultrasonic-assisted method	11
D.	Hydrothermal and solvothermal method	12
1.2.2	Optical properties of CQDs	13
1.2.2.1	Absorption	13
1.2.2.2	Fluorescence	13
1.2.2.3	Phosphorescence	17
1.2.3	The influence of doping on the fluorescence properties of CQDs	17
1.2.3.1	Single-heteroatoms doping	18
A.	N-Doped CQDs	18
B.	S-Doped CQDs	19
C.	B-Doped CQDs	20
D.	P-Doped CQDs	20
1.2.3.2	Co-doping of multi heteroatoms	21
A.	N and S co-doped CQDs	22
B.	N and P co-doped CQDs	22
C.	N and B co-doped CQDs	23
D.	B and S co-doped CQDs	24
1.3	Fluorescence quantum yield	24
1.4	An overview of Fluorescence quenching	24
1.5	Applications of CQDs	26
1.5.1	Biosensing	26
1.5.2	Chemical sensing	27
1.5.3	Photocatalysis	28
1.5.4	Bio-imaging	29

1.5.5	Drug delivery	30
1.5.6	Optoelectronics	32
1.5.7	Peroxidase-like mimetic activity	33
1.6	Motivation of the study	34
1.7	Objectives of the study	35
Chapter 2: Materials and Methods		37-53
2.1	Introduction	37
2.2	Materials	37
2.3	Methods	39
2.3.1	Synthesis of carbon quantum dots (CQDs)	39
2.4	Preparation of standard	40
2.4.1	Preparation of standard solution of ascorbic acid (AA)	40
2.4.2	Preparation of standard solution of 3,3',5,5'-Tetramethylbenzidine (TMB)	40
2.4.3	Preparation of standard solution of Picric Acid (PA)	40
2.4.4	Preparation of standard solution of chlorpyrifos	41
2.5	Biocompatibility and Cell Viability studies	41
2.6	Calculations	41
2.6.1	Quantum yield (QY) determination	41
2.6.2	Determination of limit of detection (LOD)	42
2.6.3	Determination of Stern-Volmer constant	42
2.7	Characterization of CQDs	42
2.7.1	Transmission Electron Microscopy (TEM)	42

2.7.2	Fourier Transform Infrared Spectroscopy (FTIR)	44
2.7.3	UV-visible Spectroscopy	45
2.7.4	Fluorescence Spectroscopy	48
2.7.5	X-ray Diffraction (XRD)	49
2.7.6	Zeta Potential	51
2.7.7	X-ray Photoelectron Spectroscopy (XPS)	52
Chapter 3:		54-81
Mustard seeds derived fluorescent carbon quantum dots and their peroxidase-like activity for colorimetric detection of H₂O₂ and ascorbic acid in a real sample		
3.1	Introduction	54
3.2	Materials and method	56
3.2.1	Hydrothermal Synthesis M-CQDs	56
3.2.2	Quantum yield determination	56
3.2.3	Investigation of Peroxidase- like mimetic activity	57
3.2.4	Analysis of hydroxyl radical	57
3.2.5	Detection of H ₂ O ₂ by colorimetric method	58
3.2.6	Detection of Ascorbic Acid (AA)	58
3.2.7	Colorimetric detection of AA in real fruit juices	58
3.2.8	Experimental methodology	58
3.3	Results and discussion	59
3.3.1	Characterization	59
3.3.2	Photophysical properties	62
3.3.3	Peroxidase-like mimetic activity of M-CQDs	65

3.3.3.1	Steady-state kinetic assay of M-CQDs	67
3.3.3.2	Possible Mechanism of peroxidase-like mimetic activity	71
3.3.3.3	Colorimetric detection of H ₂ O ₂	73
3.3.3.4	Colorimetric detection of ascorbic Acid	74
3.3.3.5	Colorimetric detection of AA in real fruits Juices	78
3.4	Conclusion	80
Chapter 4:		82-103
Nitrogen/sulfur-co-doped carbon quantum dots: a biocompatible material for the selective detection of picric acid in aqueous solution and living cells		
4.1	Introduction	82
4.2	Materials and method	84
4.2.1	Synthesis of NS-CQDs	84
4.2.2	Assay for the detection of PA	85
4.2.3	Cell Culture	85
4.2.4	Cytotoxicity study of NS-CQDs	85
4.2.5	Quantification of cellular fluorescence	86
4.2.6	Quantum yield determination	86
4.2.7	Experimental methodology	87
4.3	Results and discussion	87
4.3.1	Characterization	87
4.3.2	Optical Properties	92
4.3.3	Selectivity towards the detection of PA	95
4.3.4	Sensitivity assay	96

4.3.5	Possible mechanism of PA sensing	98
4.3.6	Biocompatibility & Cell Viability	100
4.3.7	Picric acid sensing in living cells	101
4.4	Detection of PA in a real environmental sample	102
4.5	Conclusion	103
Chapter 5:		104-128
Synthesis of fluorescent carbon quantum dots from Jatropha fruits and their application in fluorometric sensor for the detection of chlorpyrifos		
5.1	Introduction	104
5.2	Materials and method	107
5.2.1	Synthesis of J-CQDs	107
5.2.2	Assay for AChE activity	108
5.2.3	Detection of chlorpyrifos	108
5.2.4	Experimental methodology	109
5.2.5	Quantum yield determination	109
5.3	Results and discussion	109
5.3.1	Characterizations	109
5.3.2	Optical Properties	112
5.3.3	Detection assay of chlorpyrifos	116
5.3.4	Detection of chlorpyrifos	119
5.3.5	Selectivity of chlorpyrifos	122
5.3.6	Possible Mechanism	123
5.4	Real Sample Analysis	127
5.5	Conclusion	127

Summary	128-131
Future Recommendations	132-133
References	134-171
List of publications	172-174

List of Figures

Figure No.	Title	Page No.
Figure 1.1	Structure of few carbon-based nanomaterials	4
Figure 1.2	Illustration of fluorescence and phosphorescence in a Jablonski diagram	14
Figure 1.3	A reduction in nanoparticle size increases their energy band gap, resulting in different-coloured nanoparticles	15
Figure 2.1	Schematic representation of working of Transmission electron microscopy (TEM)	43
Figure 2.2	Photograph of Transmission electron microscopy (TEM)	44
Figure 2.3	Illustration of the FT-IR process and its photographs	45
Figure 2.4	Schematic of Possible Electronic Transitions in UV-visible Spectroscopy	47
Figure 2.5	Illustration of working principle and photograph of UV-visible spectroscopy	47
Figure 2.6	Fluorescence spectrophotometer working principle diagram	49
Figure 2.7	A photo of a fluorescence spectrophotometer	49
Figure 2.8	Schematic illustration of X-ray diffraction by crystal planes	50
Figure 2.9	The working principle of Zetasizer and its photograph	51
Figure 2.10	Working principle of X-ray photoelectron spectroscopy (XPS)	53
Figure 2.11	Typical photograph of XPS instrument	53
Figure 3.1	(a) TEM micrograph and SAED (inset) of M-CQDs (b) Size distribution (c) P-XRD pattern and (d) FT-IR spectra of as-synthesized M-CQDs	60
Figure 3.2	Zeta potential profile of as-synthesized M-CQDs	61
Figure 3.3	(a) XPS survey spectrum (b) C1s (c) N 1s and (d) O 1s spectra of as-synthesized M-CQDs	62
Figure 3.4	(a) UV-visible absorption spectrum and (b) Excitation dependent emission spectrum of synthesized M-CQDs	63
Figure 3.5	Absorbance of M-CQDs at different pH with corresponding photograph under UV- light ($\lambda_{ex}= 365$ nm)	64
Figure 3.6	(a) Ionic stability of M-CQDs in different concentration of KCl solution with image under UV-Light ($\lambda_{ex}= 365$ nm) (b) Photostability of M-CQDs	65

	after exposure of normal light for 8 h (red line) with initial absorbance (black line)	
Figure 3.7	UV- visible absorption spectrum of different system in 0.2 M acetate buffer at pH 4, bare TMB (black line), TMB+H ₂ O ₂ (red line) and TMB+H ₂ O ₂ +M-CQDs (blue line) with color change (inset Figure).	66
Figure 3.8	Optimization parameter for the oxidation of TMB by M-CQDs at different (a) pH (b) temperature (c) time (d) Concentration of H ₂ O ₂ and (e) Concentration of TMB	67
Figure 3.9	Steady-state kinetic assay of the M-CQDs, where the velocity was determined through oxidation of TMB with the corresponding absorption at 652 nm with varying concentrations of (a) TMB and (d) H ₂ O ₂ and the corresponding Lineweaver–Burk plots obtained through fixed the concentration of one with varying the other substrate: (b) Varying the TMB at a fixed H ₂ O ₂ concentration and (e) Varying the H ₂ O ₂ at a fixed TMB concentration, along with the double reciprocal plots: (c) Varying the TMB with keeping H ₂ O ₂ constant and (f) Varying the TMB, H ₂ O ₂ while keeping constant.	70
Figure 3.10	(a) Control experiment in the oxidation of TMB in the presence of [•] OH radical scavenger isopropyl alcohol (IPA) and methyl alcohol (MA). (b) Fluorescence spectra of terephthalic acid in the presence of H ₂ O ₂ and different concentration of M-CQDs indicate the involvement of [•] OH radical.	71
Figure 3.11	(a) Colorimetric detection of H ₂ O ₂ with corresponding color change (b) Change in absorption at 652 nm in the presence of different concentration of H ₂ O ₂ with inset graph shows linear range 0.02-0.2 mM of detection limit 0.015 mM.	73
Figure 3.12	(a) ox-TMB based colorimetric detection of ascorbic acid (AA) (b) Change in absorption at 652 nm in the presence of different concentration of AA in the liner range (10 to 70 μM).	76
Figure 3.13	Change in fluorescence of M-CQDs in the presence of TMB (red line), TMB+H ₂ O ₂ (blue line) and TMB+H ₂ O ₂ +AA (green line) along with colour change (inset photograph).	77
Figure 3.14	Selectivity test of AA detection by ox-TMB in the presence of common reducing agents	78
Figure 3.15	Practical feasibility of AA detection by ox-TMB in real sample <i>viz.</i> common fruits juice along with photograph of different fruit juice (A).	79
Figure 3.16	Interference test of AA detection in real sample	80
Figure 4.1	TEM micrograph of synthesized NS-CQDs with insect SAED image (a), Average size distribution histogram (b), P-XRD pattern, and (c) FT-IR	89

	spectrum of NS-CQDs.	
Figure 4.2	Zeta potential summary of as-synthesized NS-CQDs	90
Figure 4.3	XPS wide scan spectrum of synthesized NS-CQDs	90
Figure 4.4	XPS spectra of (a) C1s (b) N1s (c), O1s spectra (d), and S2p NS-CQDs	92
Figure 4.5	UV-visible absorption spectrum (black line) and Fluorescence spectrum (blue line) at the excitation of 360 nm (a), CIE Co-ordinates images shows the blue color of NS-CQDs (b) Fluorescence emission spectra show at the different excitation wavelength (240-400 nm) (c), represents the fluorescence intensity at different pH range from 2 to 12 (d).	94
Figure 4.6	(a) Effect of fluorescence emission on adding different NaCl concentration. (b) Effect of fluorescence emission after 5 months of incubation at 5 °C.	95
Figure 4.7	(a) Selectivity test of NS-CQDs for PA in the co-existence of different nitro and non-nitro explosives (concentration of PA and another explosive was 100 µM in 0.2 M sodium acetate buffer at pH 2), (b) Shows the interference study in different metal ions towards the PA detection, whereas, F_0 and F are the fluorescence emission intensity before and after the addition of various analytes	96
Figure 4.8	(a) Fluorescence emission intensity on increasing the concentration of PA from 0-200 µM (b) Shows the linear calibration graph between the concentration ranges of 0-3 µM	97
Figure 4.9	(a) Represents the overlapping of the absorption spectrum of PA with the emission and excitation of NS-CQDs, (b) shows the time resolve fluorescence spectra of NS-CQDs with and without PA	99
Figure 4.10	Zeta potential of NS-CQDs after the addition of PA	100
Figure 4.11	(a) The HeLa cells incubated with increasing concentrations of the NS-CQDs were quantified for fluorescence intensity as a measure of NS-CQDs uptake and staining. The intracellular fluorescence intensity was depicted as fold fluorescence in the form of a bar graph, (b) The HeLa cells were exposed to a variable concentration of the NS-CQDs, and the degree of cellular viability was estimated using MTT assay. The detected absorbance was represented as percent cell viability.	101
Figure 4.12	Graph depicting decreasing fold fluorescence in pre-treated cells when subjected to increasing concentration of PA	102
Figure 5.1	(a) TEM micrograph of synthesized J-CQDs with insect SAED image. (b) Average size distribution histogram. (c) P-XRD pattern and (d) FT-IR spectrum of J-CQDs	110

Figure 5.2	The hydrodynamic size of as-synthesized J-CQDs	111
Figure 5.3	(a) XPS spectra of J-CQDs, wide range spectra (b) C1s (c) N1s and (d) O1s spectra	112
Figure 5.4	(a) UV-visible absorption spectrum and (b) different excitation (300- 510 nm) dependent emission spectrum of synthesized J-CQDs. (c) CIE color Coordinate (0.16, 0.17) diagram of J-CQDs is showing blue color (d) Effect of different pH, on the emission of J-CQDs	114
Figure 5.5	Effect of emission spectra of J-CQDs on adding different NaCl concentration	115
Figure 5.6	Effect of fluorescence intensity after 8 months of incubation at 5 °C	115
Figure 5.7	(a) UV-visible spectrum of J-CQDs+DTNB, J-CQDs+DTNB+ATCh, J-CQDs+DTNB+ATCh+ AChE and J-CQDs+DTNB+ATCh+AChE+Cpf system (b) fluorescence spectrum	117
Figure 5.8	(a) Represents the emission intensity of ATCh + J-CQDs + DTNB system on varying AChE concentration from 0 to 100 mU/mL, (b) corresponding fluorescence change in a linear range of 30-80 mU/mL	117
Figure 5.9	Influence of (a) ATCh, [0.1-1.0 mol/L] (b) AChE, [20-120 mU/mL] (c) DTNB [0.1-1.0 mol/L] and (d) Cpf [2-12 µg/ mL] on emission intensity of J-CQDs [4 µg/mL]	118
Figure 5.10	Influence of Cpf concentration on IE of reaction system J-CQDs + DTNB + ATCh + AChE at (a) different pH [2-12], (b) different temperature, and (c) different incubation time; [Cpf = 0.2 µg/mL].	119
Figure 5.11	(a) Fluorescence emissions at 462 nm in the presence of various concentration of Cpf (0-1 µg/mL) in J-CQDs + DTNB + ATCh + AChE system, and also showing snap shot with increasing concentration from 0 to 1 µg/mL (b) Linear plot between IE and Cpf concentration (0.02-0.18 µg/mL).	120
Figure 5.12	Inhibition efficiency (IE) of different OPs including chlorpyrifos (Cpf), profenofos (Pro), malathion (Mal), and glyphosphate (Gly), [OPs] = 0.2 µg/mL.	122
Figure 5.13	(a) Represents the selectivity among different metal ions and various other amino acids (100 µL, 4 µg/mL), biomolecules (100 µL, 4 µg/mL) and cpf (100 µL, 0.2 µg/mL) in sensing system of J-CQDs + ATCh + ATChE + DTNB (b) Interference study of different metal ions (100 µL, 4 µg/mL) in J-CQDs + ATCh + ATChE + DTNB+Cpf system and various other molecules in the presence of Cpf (100 µL, 0.2 µg/mL)	123
Figure 5.14	(a) Represents the emission spectra of J-CQDs on increasing the concentration of TNBA (b) Shows the fluorescence time resolved spectra of	124

	J-CQDs before and after addition of TNBA	
Figure 5.15	Zeta potential of the synthesized J-CQDs and TNBA	124
Figure 5.16	Absorbance spectra of J-CQDs, TNBA and J-CQDs and TNBA mixture	125
Figure 5.17	Overlapped absorbance spectra of TNBA on excitation and emission spectra of J-CQDs	126

List of Schemes

Scheme No.	Title	Page No.
Scheme 1.1	An illustration of the techniques associated with the synthesis of fluorescence CQDs	7
Scheme 3.1	Illustration of the hydrothermal synthesis of carbon quantum dots by mustard seeds.	56
Scheme 3.2	The possible mechanism in favor of peroxidase mimetic activity of M-CQDs and colorimetric detection of H ₂ O ₂ and ascorbic acid.	72
Scheme 4.1	Schematic illustration of the one-step hydrothermal synthesis of NS-CQDs via TSC and CA	88
Scheme 5.1	Illustration of the one-step synthesis of J-CQDs from the Jatropha fruits	108

List of Tables

Table No.	Title	Page No.
Table 2.1	List of chemicals	37
Table 3	Fluorescence quantum yield determination of M-CQDs with reference to quinine sulphate at excitation wavelength 340 nm from the equation (2.1)	57
Table 3.1	Comparison of the Michaelis–Menten constant (K_m and V_{max}) of M-CQDs catalyzed oxidation of TMB. Where K_m is the Michaelis constant and V_{max} is the maximum velocity	69
Table 3.2	Comparison of colorimetric detection of H_2O_2 by M-CQDs with HRP and Carbon based nanoprobe	74
Table 3.3	Comparison of AA detection by M-CQDs with HRP and carbon based different optical sensors	75
Table 4.1	Fluorescence QY determination of NS-CQDs with reference to quinine Sulfate at excitation wavelength 360 nm	86
Table 4.2	Comparison table for the PA detection with the earlier reported materials	97
Table 4.3	Fitting data of fluorescence lifetimes for the NS-CQDs and the NS-CQDs+PA hybrid.	99
Table 4.4	Standard recovery experiment after spiking with PA of different concentration in the pond water sample	103
Table 5.1	Comparison of different method with our synthesized nano-probe for the detection of Cpf.	121
Table 5.2	Recovery experiment for the detection of Cpf into natural samples	127

List of Symbols/Abbreviations

PA	Picric acid
TNT	Trinitro Toluene
c	Concentration absorbing molecule in mol.m ⁻³
FRET	Fluorescence resonance electron transfer
IFE	Inner filter effect
AuNPs	Gold nanoparticles
CIE	Commission Internationale de l'Éclairage
TRV	Toxicity Reference Value
LED	Light emitting diode
CNTs	Carbon nanotubes
LOAEL	Lowest observed adverse effect level
CQDs	Carbon quantum dots
N-CQDs	Nitrogen doped-CQDs
S-CQDs	Sulfur doped-CQDs
B-CQDs	Boron doped-CQDs
P-CQDs	Phosphorous doped-CQDs
NS-CQDs	Nitrogen sulfur co-doped CQDs
d	Interplanar spacing
HRP	Horseradish peroxidase
EDAX	Energy-dispersive X-ray spectroscopy
et al.	Co-authors
FT-IR	Fourier transform infrared spectroscopy
FL	Fluorescence
AA	Ascorbic acid
H₂O₂	Hydrogen peroxide
Phe	Phenol
NB	Nitrobenzene
2-CP	2-chlorophenol
2,4-DNP	2,4-dinitrophenol
Res	Resorcinol

IB	Iodobenzene
BB	Bromobenzene
1,3-DNB	1,3-dinitrobenzene
4-NP	4-nitrophenol
2-NP	2-nitrophenol
NaAc	Sodium acetate
I_0	Intensity of the incident radiation
RT	Room temperature
I_t	Intensity of the transmitted radiation
JCPDS	Joint committee on powder diffraction standards
LED's	Light emitting diodes
LOD	Limit of detection
RSD	Relative standard deviation
MRI	Magnetic resonance imaging
MTT	3-(4, 5-dimethylthiazol-2-yl)-2, 5-diphenyl-tetrazolium bromide
NaAc	Sodium acetate buffer
TSC	Thiasemicarbazide
oxTMB	Oxidized TMB
PBS	Phosphate buffer saline
XPS	X-ray photoelectron spectroscopy
TEM	Transmission Electron Microscopy
K_m	Michaelis-Menton constant
V_{max}	Maximum velocity
V	Initial velocity
QY	Quantum yield
QS	Quinine sulfates
R²	Correlation coefficient
SAED	Selected area diffraction pattern
t	Time (min)
IPA	Isopropyl alcohol

TPA	terephthalic acid
MA	Methyl alcohol
TiO₂	titanium oxide
CA	Citric acid
TMB	Tetramethylbenzidine
TA	Terephthalic acid
M-CQDs	Mustard carbon quantum dots
GO	Graphene oxide
XRD	X-ray diffraction spectroscopy
ϵ	Molar absorption coefficient
θ	Angle (degree)
λ	Wavelength
OPs	Organophosphates
Cpf	Chlorpyrifos
AChE	Acetylcholinesterase
ATCh	Acetylcholine
TCh	Thiocholine
TNBA	5-thio-2-nitrobenzoic acid
DTNB	5,5-dithiobis (2-nitrobenzoic acid)

Preface

This thesis describes the development of different kinds of carbon-based nanomaterials, which is synthesized from natural and organic carbon precursors for the detection of biosensors, pesticides and hazardous nitro compounds etc. These fluorescence small carbon nanoparticles have a particle size of less than 10 nm and are a promising nano-biotechnology material due to their smaller particle size, excellent biocompatibility, large surface and high surface energy, high quantum yield, excitation dependent photoluminescence behaviour, high water solubility, ease of production, and low toxicity. Due to their unique physicochemical, optical and electronic properties, these materials are a rising star in various fields such as biosensing, bioimaging, drug delivery, optoelectronics, photovoltaics, and photocatalysis. To improve their functionality and optical properties, CQDs have been synthesized from natural and chemical precursors using laser ablation, arc discharge, chemical oxidation, electrochemical oxidation, hydrothermal carbonization, and microwave irradiation. Among them are laser ablation and arc discharge, which require sophisticated and expensive equipment, as well as chemical oxidation and electrochemical oxidation, which require strong acids. While microwave irradiation provides an easy method for synthesizing CQDs within minutes, it is limited by its uncontrollable reaction conditions. It is common to choose the hydrothermal route currently due to its simplicity, rapidity, controlled reaction conditions, and cost-effectiveness. In addition, CQDs can also be synthesized using natural carbon sources due to their low cost, environmental friendliness, and widespread availability. There have been numerous studies using natural carbon sources, such as mustard seeds, soybeans, orange peel juice, green grass, milk, potatoes, plant leaves, soy milk, cocoon silk, and so forth, to synthesize CQDs. Various organic compounds have been

Preface

also used in the synthesis of CQDs, such as ascorbic acid, tartaric acid, citric acid, glycol, glucose, sucrose, and glycerol. Nevertheless, the primary challenge remains to develop CQDs that produce high quantum yields (QY).

Chapter 1 cover the basics of nanotechnology, its origins in brief, and the different types of nanomaterials. In addition to this, the section also contains a brief history of previous and ongoing research on the synthesis of CQDs and their applications. The goals and scope of the present investigation have been outlined at the end of this chapter.

Chapter 2 In this section, the experimental details, including the materials and instruments that have been used to fully characterize the carbon quantum dots, are discussed. In this chapter, the preparation of standard solutions and various calculations are also covered, such as quantum yields, quenching constants, and limit detection of detections.

Chapter 3 summarized the synthesis of fluorescent carbon quantum dots via facile one-step hydrothermal treatment of mustard seeds (M-CQDs). It showed excellent optical property with fluorescent quantum yield 4.6 %. The as-prepared M-CQDs exhibited peroxidase-like mimetic activity and catalyzed the oxidation of chromogenic substrate 3,3',5,5'-tetramethylbenzidine (TMB) in the presence of H₂O₂ to produce a blue color reaction mixture with the prominent peak at 652 nm. Furthermore, the peroxidase-like activity performance of M-CQDs followed the steady-state kinetics behavior and exhibited similar catalytic activity as that of natural enzyme Horseradish peroxidase (HRP). In addition to this, the double reciprocal plot showed a parallel line which suggested the occurrence of Ping-Pong

Preface

type of mechanism. The H_2O_2 dependent oxidation of TMB was helpful for the colorimetric detection of H_2O_2 in the linear range of 0.02 to 0.20 mM with the limit of detection (LOD) of 0.015 mM. Interestingly, the oxidized TMB was further reduced to native TMB by the reducing agent ascorbic acid. Hence M-CQDs showed its potential towards the selective and sensitive detection of ascorbic acid in the linear range of 10 to 70 μM having a correlation coefficient of 0.998 with LOD of 3.26 μM . The practical feasibility of the proposed detection method of AA was also investigated in common fresh fruits.

Chapter 4 the present study aims the development of hazardous explosive picric acid sensor based on the NS-CQDs. In this work, we utilize a one-pot hydrothermal technique for the synthesis of nitrogen/sulfur-co-doped fluorescent carbon quantum dots (NS-CQDs) from citric acid (CA) and thiosemicarbazide (TSC). The obtained NS-CQDs exhibited strong blue emission under UV light, with fluorescence quantum yield (QY) of ~37.8%. The Commission internationale de l'éclairage (CIE) coordinates originated at (0.15, 0.07), which confirmed the blue fluorescence of the synthesized NS-CQDs. Interestingly, the prepared NS-CQDs were successfully used as a selective nanoprobe for the monitoring of environmentally hazardous explosive picric acid (PA) in different nitro- and non-nitro-aromatic derivatives of PA. The mechanism of the NS-CQDs was also explored, and was posited to occur via the fluorescence resonance electron transfer (FRET) process and non-fluorescent complex formation. Importantly, this system possesses excellent biocompatibility and low cytotoxicity in HeLa cervical cancer cells; hence, it can potentially be used for PA detection in analytical, environmental, and pathological applications. Furthermore, the practical applicability of the proposed

Preface

sensing system to pond water demonstrated the feasibility of our system along with good recovery.

Chapter 5 reports the green synthetic method for the synthesis of water-soluble fluorescent CQDs. Now a days, green route are significantly favoured for the synthesis of CQDs, which develop the use of natural renewable carbon sources. The use of green sources has several advantages due to zero cost, non-toxicity, environmental friendliness, and easy availability. In this study, we have synthesized fluorescent carbon quantum dots (J-CQDs) from Jatropha fruit by using a one-pot hydrothermal approach, for the first time. The as-synthesized J-CQDs exhibited bright blue fluorescence emission with a high quantum yield of 13.7 %. Furthermore, the synthesized fluorescent J-CQDs have been used as a fluorometric sensor for the detection of pesticides. The sensing of pesticides is based on the irreversible catalytic inhibition of acetylcholinesterase (AChE) enzyme with a controlled fluorescence quenching process. The thiocholine was mainly triggered by the decomposition of DTNB to form yellow-colored TNBA. Further, TNBA gradually quenched the fluorescence emission spectra of added J-CQDs via electron transfer process. The catalytic activity of AChE was inhibited in the presence of OPs, leading to the recovery of the fluorescence signal. Thus, a sensitive and selective nanoprobe was designed for the sensing of OPs (chlorpyrifos) along with a detection limit 2.7 ng/mL. Apart from this, the proposed sensing method has been successfully applied for pesticide detection in environmental and agricultural samples with acceptable recovery. Thus, the delivered result suggests that our probe is simple in design, having a short reaction time, and could be proficiently used in further analytical and environmental applications in the future.